ACS OMEGA

http://pubs.acs.org/journal/acsodf

Article

Anti-Biofouling Features of Eco-Friendly Oleamide–PDMS Copolymers

Eunseok Seo, Myeong Ryun Seong, Ji Woong Lee, Heejin Lim, Jiwon Park, Hyungbin Kim, Hyundo Hwang, Dohoon Lee, Jiho Kim, Gwang Hoon Kim, Dong Soo Hwang, and Sang Joon Lee*

Cite This: *ACS Omega* 2020, 5, 11515–11521

Read Online

ACCESS | Metrics & More | Article Recommendations | Supporting Information

ABSTRACT: The biofouling of marine organisms on a surface induces serious economic damage. One of the conventional anti-biofouling strategies is the use of toxic chemicals. In this study, a new eco-friendly oleamide–PDMS copolymer (OPC) is proposed for sustainable anti-biofouling and effective drag reduction. The anti-biofouling characteristics of the OPC are investigated using algal spores and mussels. The proposed OPC is found to inhibit the adhesion of algal spores and mussels. The slippery features of the fabricated OPC surfaces are examined by direct measurement of pressure drops in channel flows. The proposed OPC surface would be utilized in various industrial applications including marine vehicles and biomedical devices.

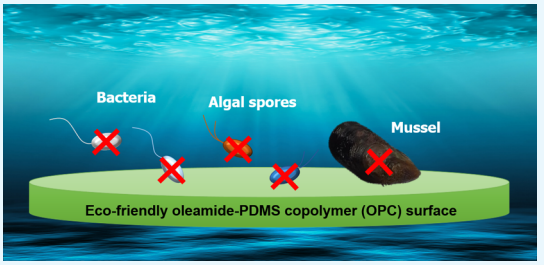

1. INTRODUCTION

Marine biofouling indicates the accumulation of undesirable foulants, such as microorganisms, seaweeds, and sea animals, on object surfaces immersed under the sea.[1] Marine biofouling involves the initial bacterial attachment and the formation of a biofilm on the surface, followed by the attachment of larger marine organisms. Biofilms contaminate a wide variety of infrastructural elements, systems, and devices. The fouling of ship hulls and ocean structures incurs huge costs through increased maintenance cost and additional fuel consumption because of the increased frictional drag and increased frequency of dry-docking for the removal of fouling organisms in compliance with the enhanced marine environmental regulations.[1−9] During the past decades, numerous studies have been devoted to develop effective antifouling and drag reduction methods.[10−16] Despite extensive efforts to develop various anti-biofouling materials, the effective prevention of biofilm formation remains challenging. Among the solutions suggested for combating marine biofouling, the self-polishing coating system containing tributyltin (TBT) is proven to be one of the most effective methods. However, conventional antifouling agents, such as the TBT biocidal coatings, are toxic. TBT has been banned worldwide by the International Maritime Organization because of its negative environmental effects associated with toxicity.[15,17,18] In addition, conventional toxic coatings will be totally banned in the near future because of the gradually enhanced marine environmental regulation. Thus, new studies on the developments of biomimetic surfaces and natural compounds inspired by natural systems have been receiving large attention nowadays because of the technical limitations of conventional coatings.[16]

Nowadays, many efforts have been made to develop eco-friendly and effective antifouling materials to satisfy the demands for hindering and regulating marine biofouling.[19−28] For example, liquid-infused surfaces with drag reduction properties have been largely studied because they contain a lubricant, such as silicon oil, to make the surface slippery.[19,20] In addition, self-polishing copolymers, which maintain sustainable anti-biofouling properties, were also actively investigated.[21,22] Other polymers, such as fouling-release polymers,[23,24] zwitterionic polymers,[25,26] and protein-resistant polymers,[27,28] were used as coating materials for the fabrication of anti-biofouling surfaces.

The polydimethylsioxane (PDMS)-based material is one of the promising candidates for practical anti-biofouling applications. PDMS is a silicone material with low surface energy and can be used as a nontoxic alternative to conventional biocide paints. PDMS can lower the adhesion force acting between fouling organisms and the coating surface because of its low surface energy and small modulus,[28,29] resulting in the easy removal of organisms.[30−32]

Primary fatty acid amides, which have been used as slip agents on plastic polyethylene films and other polymers to reduce frictional resistance or to increase lubricity,[33] are commonly found in grasses, microalgae, and animals.[34] These

Received: February 11, 2020
Accepted: May 6, 2020
Published: May 15, 2020

amides use slippery surfaces to which the biofoulers are attached weakly and enhance the scratch resistance of polymer surfaces by decreasing the friction coefficient.[35] Oleamide ($C_{18}H_{35}NO$), a fatty oleic amide that is frequently used as slip agents in industrial applications, is a special antifouling compound isolated from nature.[34] Oleamide is a biologically derived substance that decomposes readily in natural environments and has strong potential as a structural material for making up bactericidal surfaces because of its intrinsic antifouling properties.[36] The surface of elastic coatings can be deformed by water movement. This elastic movement can shed the attached biofoulers under turbulent conditions.[37] Thus, the elastic and slippery oleamide surface has strong potential as an ingredient of antifouling coating materials. In this study, a new oleamide−PDMS copolymer (OPC), which utilizes both advantages of PDMS and oleamide, is proposed and its eco-friendly anti-biofouling properties are experimentally examined.

2. RESULTS AND DISCUSSION

2.1. Chemical Properties. The curing reaction of PDMS was carried out by adopting the hydrosilylation reaction method. This reaction is caused by the addition of silicon hydride to the double bond of base siloxane, with the aid of a platinum catalyst. The double bonds contained in the oleamide results in hydrosilylation reactions with silicon hydrides (Figure 1).

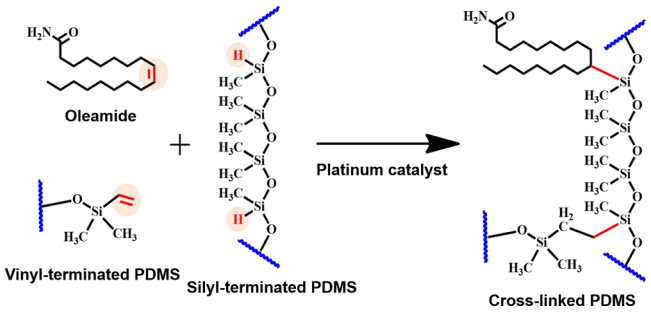

Figure 1. Schematic diagram of PDMS polymerization with oleamide.

The surface characteristics of the fabricated OPCs were analyzed using a time-of-flight secondary ion mass spectrometry (ToF-SIMS) system. Figure 2a shows spatial distribution images of oleamide ($C_{18}H_{36}NO^+$, m/z 282.30) on the OPC surfaces.[43] At a mixing ratio of 20:1, fine oleamide particles are observed to be evenly distributed on the surface. At a mixing ratio of 320:1, the size of oleamide particles is smaller than that for the 20:1 ratio and the light intensity of particles is weak because of low contents of oleamide. The concentration of oleamide shown on the OPC surface is proportional to the amount of oleamide. These surfaces might provide different surface properties, such as surface roughness, contact angle, anti-biofouling, and drag reduction effects.

Attenuated total reflection Fourier-transform infrared (ATR−FTIR) was used to obtain the chemical signatures of the PDMS and OPC surfaces. The FTIR spectra of the PDMS and OPC surfaces are displayed in Figure 2b,c. The IR band positions and attributions of PDMS were used as a base to interpret functional features of the paints polymerized with the aid of oleamide spectra. The IR band positions and attributions of PDMS were used as the base for interpreting the functional paints. The spectra are divided into two groups having similar characteristics, and they are represented by solid and dotted lines. PDMS exhibits characteristic features of the silicon network with similar Si peaks (Figure 2b). The peaks of N−H amide II, C═O amide 1, and C═O indicate the presence of oleamide (Figure 2b). As shown in Figure 2c, the broad peaks at 3358 and 3182 cm^{-1} are ascribed to the vibrations of NH_2 and OH bonds, respectively.[44] Through the interaction with surrounding water, these functional groups of the OPC surfaces may lead to the formation of the hydrophilic layer. For the cases of relatively high content of oleamide ranging from 10:1 to 80:1, the spectra are represented by solid lines in the graph. The spectra show main peaks of oleamide because they contain lots of oleamide. For the cases of relatively low levels of oleamide, including 160:1 and 320:1, and PDMS, the spectra are represented by dotted lines. The dotted lines indicated little or no content of oleamide. Thus, there are no oleamide-related peaks. The reason for the different characteristics of the spectra that appeared as the solid line and dotted line is mainly attributed to different chemical properties of the surfaces. The solid line shows the chemical properties of oleamide on the surface, while the dotted group does not. This is assumed to have an influence on the anti-biofouling effect.

2.2. Surface Characterization. The surface hardness of the PDMS and OPC surfaces fabricated at various mixing ratios was evaluated through a scratch test using a nanoindenter (Figure 3a). When the content of oleamide is low (320:1), a rigid surface is formed. However, when the content of oleamide is higher (20:1−160:1), the elasticity of the OPC surface is increased (Figure 3b). The surface of the OPC with increased elasticity becomes sticky. Notably, water sprinkled on the sticky surface results in a slippery surface (data not shown).

Figure 3c compares the wettability of the PDMS and OPC surfaces. Six different types of OPC plates were prepared with different mixing ratios of PDMS/oleamide (20:1, 40:1, 80:1, 160:1, and 320:1) to evaluate the antifouling characteristics of the OPC-coated surface. As the fraction of oleamide in the mixture increases, the water contact angle (CA) decreases. The OPC samples with mixing ratios of 160:1, 80:1, 40:1, and 20:1 are less hydrophobic compared to the PDMS and OPC 320:1 samples.

The pressure drop in channel flows over the OPC surfaces with varying Reynolds number was directly measured to examine the frictional drag reduction effect of the OPC. The drag forces exerted on the pristine PDMS and glass surfaces were measured to compare the drag reduction effect of oleamide. The measured pressure drop for the OPC surfaces mixed with ratios ranging 20:1−320:1 is smaller than that of pristine PDMS at all Re values tested (Figure 3d). This result indicates that the oleamide can give rise to less frictional drag because of the interfacial slippage. As the Reynolds number increases, the drag reduction effect of the OPC mixed at a ratio of 40:1 is increased. The drag-reduction effect of the OPC surface at Re 800 is better than that of other OPC surfaces mixed at different rates. However, the drag reduction effect is smaller than that on the glass surface. These results indicate that there is a special mixing ratio for achieving large drag reduction effects, rather than a simple increase in the content of oleamides.

2.3. Anti-Biofouling Properties. Oleamide had strong potential as a structural material for anti-biofouling surfaces because of its intrinsic antifouling properties.[33−36] Thus, the

https://dx.doi.org/10.1021/acsomega.0c00633
ACS Omega 2020, 5, 11515−11521

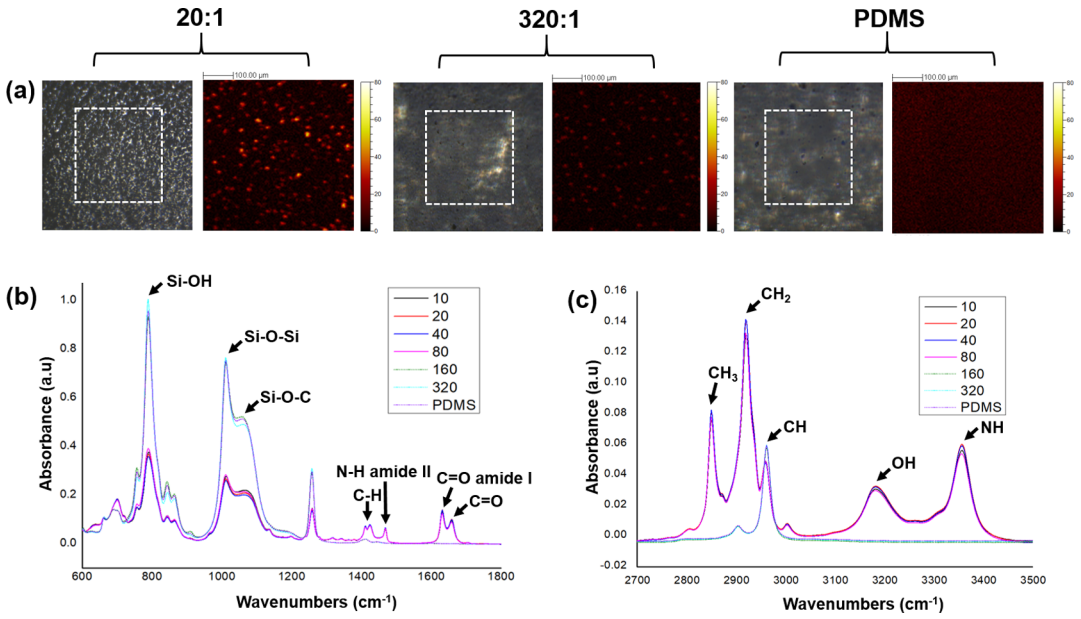

Figure 2. (a) Measurement areas of TOF-SIMS (white dashed line) and ToF-SIMS images showing spatial distribution of oleamide ($C_{18}H_{36}NO^+$, m/z 282.30). (b,c) FT-IR spectra of the PDMS and OPCs at different wavenumber ranges.

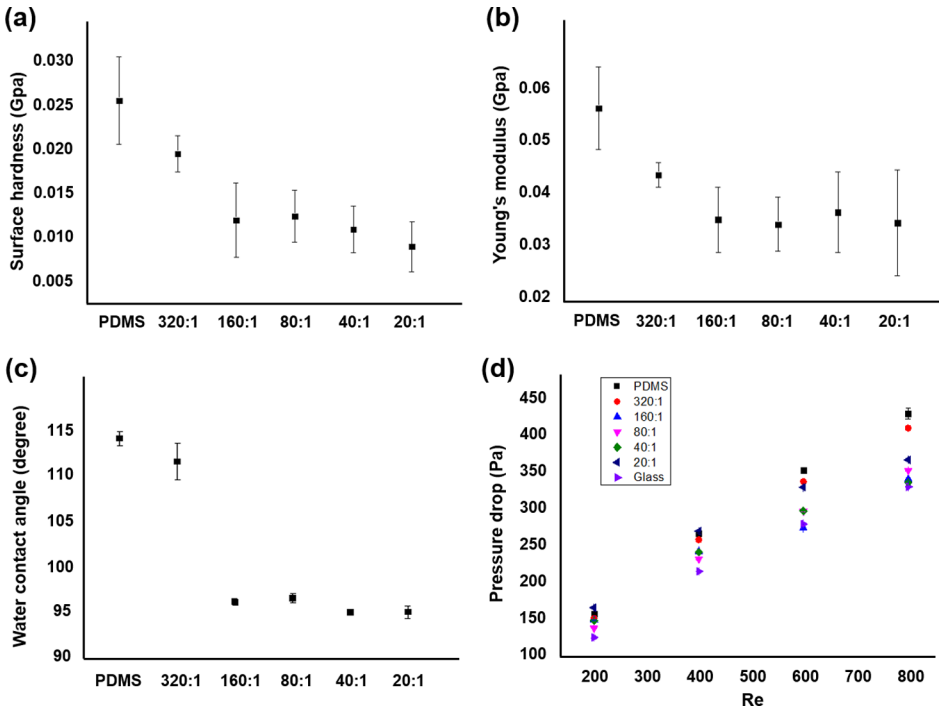

Figure 3. Comparisons of (a) surface hardness and (b) Young's modulus of the PDMS and OPC surfaces. N = 25. (c) Contact angles of the fabricated OPCs. N = 5. (d) Effect of the content of oleamide on the pressure drop of the OPC surfaces attached to the channel bottom according to the Reynolds number. N = 3.

anti-biofouling features of the submerged OPC surfaces were evaluated using algal spores. The biofouling properties of the pristine PDMS and the proposed OPC surfaces containing different amounts of oleamide were tested by exposing the test surfaces to algal spores and capturing optical images. As illustrated in Figure 4a, a large number of laver spores (*Pyropia yezoensis*) are adhered to the control PDMS sample, whereas the number of laver spores on the OPC surfaces is very few. As show in Figure 4b, the anti-biofouling effect is enhanced as the amount of oleamide contained in OPC increases. These results demonstrate that the fabricated OPC surfaces have excellent antifouling features. Thus, the proposed OPC can be applied to various industrial applications that require strong anti-biofouling surfaces.

2.4. Mussel Antifouling Assay. The effects of surface chemistries on the settlement and dynamic behaviors of mussels were studied in a tank of seawater.[45] After the deposition of mussels on the surface of a polystyrene Petri dish located in a tank of seawater, the mussels interact continuously with the floor surface. In addition, the foot is freely stretched

https://dx.doi.org/10.1021/acsomega.0c00633
ACS Omega 2020, 5, 11515−11521

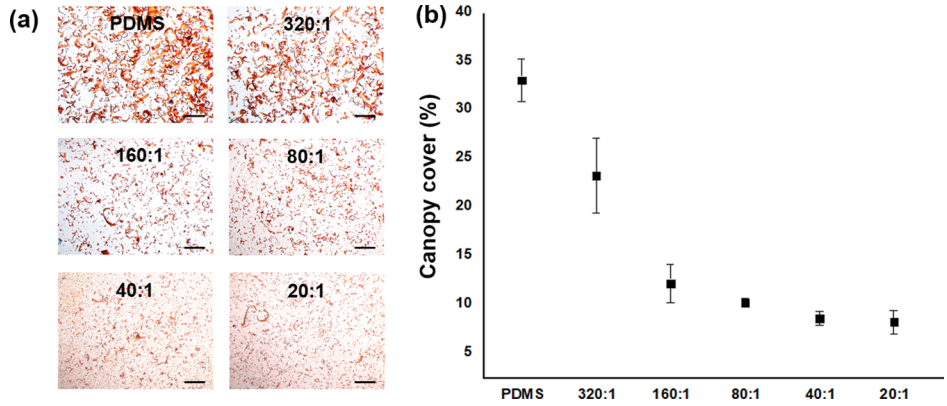

Figure 4. (a) Typical images of red algal (*P. yezoensis*) spores cultured on the PDMS and OPC surfaces. (b) Variation of canopy cover showing the number of red algal spores cultured on the PDMS and OPC surfaces for 3 weeks. Scale bars = 2 mm.

out of the body and repeatedly landed on the floor (Figure 5A, also shown in Movie S1).

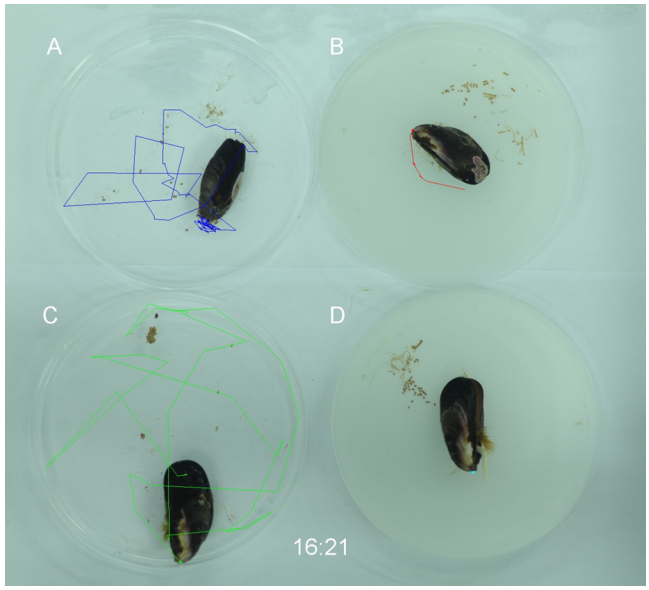

Figure 5. Dynamic movements of four mussels were monitored for more than 16 h on the surfaces of (A) polystyrene, (B) 20:1 (24 h) OPC, (c) PDMS, and (D) 20:1 (6 h) OPC.

The mussels deposited in a tank with OPC 20:1 (24 h) do not interact with the dish floor and the foot of the mussel. The mussel frequently stretches its foot out of the body, and the body slightly moves. However, it failed to interact with the floor surface (Figure 5B, also shown in Movie S1).

After the deposition of mussel on the PDMS surface, the mussel is initially standing on the edge blade while moving its foot. Thereafter, the mussel foot tries to move toward the wall. Throughout the 16 h observation, mussels are observed to primarily move around the wall, interacting with the wall (Figure 5C, also shown in Movie S1).

The mussels deposited in a tank with OPC 20:1 (6 h) do not interact with the dish floor and the foot of the mussel. The mussel frequently stretches its foot out of the body but fails to interact with the floor surface. The foot is consistently coming out but cannot reach the surface. The mussel does not move at all for 16 h (Figure 5D, also shown in Movie S1). These results demonstrate that the OPC has excellent antifouling features for mussels.

To apply the OPC to the surface coating of marine vehicles and equipment, a sustainable technology that can sustain the anti-biofouling effect of oleamide as long as possible should be developed. Thus, in the near future, systematic durability testing is required to verify how long oleamide does not fall off from the OPC surface under the marine environment. In the fabrication of the OPC surface, the effects of the addition of antioxidants or polymerization with other polymers and oleamides have to be assessed. The development of advanced functional surfaces is also needed to enhance the anti-biofouling and drag reduction effects. In the manufacturing process, we need to find a suitable hardening method that can work at room temperature for practical coating of marine vehicles. In addition, the cytotoxicity of the copolymers should be assessed for practical application to biomedical devices.

3. CONCLUSIONS

In this study, the fabricated OPC surfaces were found to protect from the biofouling induced by laver spores and mussels. These results imply that the OPC can be used as an eco-friendly antifouling agent for preventing the settlement of foulants. In addition, the direct measurement of frictional drag exerted on the proposed OPC shows that oleamide has a strong positive influence on drag reduction. The proposed bioinspired OPC would be effectively utilized in various industrial applications including marine, biomedical, and water management.

4. EXPERIMENTAL SECTION

4.1. Materials. The Sylgard 184 PDMS silicone elastomer was purchased from Dow Corning Co., Ltd. The analytical-grade oleamide was obtained from Tokyo Chemical Industry Co., Ltd. Other reagents were obtained from Sigma-Aldrich.

4.2. Fabrication of the OPC. As a control sample, a mixture of the PDMS prepolymer and a curing agent (10:1 by weight) was first poured onto a plate. To fabricate OPC test samples, a mixture of the PDMS prepolymer and a curing agent was mixed with oleamide solution (in toluene) at weight ratios in the range of 10:1−320:1 (PDMS mixture/oleamide). The prepared mixtures were poured quickly onto a plate and allowed to solidify in an oven maintained at 60 °C for 24 h (Figure S1).

https://dx.doi.org/10.1021/acsomega.0c00633
ACS Omega 2020, 5, 11515−11521

4.3. Time-of-Flight Secondary Ion Mass Spectrometry. Chemical properties of the fabricated OPC surfaces were evaluated by ToF-SIMS. The ToF-SIMS analysis was conducted using a ToF-SIMS 5-100 system (ION-TOF, Münster, Germany) using a pulsed 30 keV Bi_3^+ primary ion beam in the spectrometry mode for positive ions. Low-energy electrons were applied onto the surface of the test samples with an electron flood gun for charging compensation during the analysis. ToF-SIMS images were captured over an area of 500 × 500 μm^2 with 128 × 128 pixels under the positive mode. The Bi_3^+ current was typically 0.5 pA for the spectrometry mode. Internal mass calibration for ToF-SIMS spectra was conducted at the H^+, H_2^+, CH_3^+, and $C_2H_3^+$ peaks in the positive ion mode before further detailed analysis.

4.4. ATR−FTIR Analysis. The chemical composition of the fabricated OPC surfaces was examined using an ATR−FTIR spectroscope. ATR−FTIR experiments were performed at the 12D IRS beamline of Pohang accelerator laboratory. The FTIR spectra were obtained using the VERTEX 80V spectrometer (Bruker) attached with an ATR accessory (PIKE Technologies). The spectra were recorded at a 4 cm^{-1} spectral resolution using a deuterated triglycine sulfate detector under a vacuum condition.[38]

4.5. Surface Characterization. The mechanical properties, including surface hardness and Young's modulus, of the PDMS and OPC surfaces fabricated at various mixing ratios were measured through a scratch test using a nanoindenter (Nano Indenter XP, MTS Systems Corporation).[39]

The CA was measured to evaluate the wetting properties of the fabricated OPC surfaces. The static CA of a 3 μL water droplet was measured using a video-based optical system (FAMTOFAB SDL-TEZD, Korea) to analyze the wettability of the fabricated OPC surfaces. The CA of each sample surface was measured five times repeatedly at five random points. The measured CA values were averaged.

Pressure drops in a rectangular PDMS microfluidic channel (length: 70 mm, width: 4 mm, and height: 0.6 mm) were measured to estimate the frictional drag exerting on the fabricated OPC surfaces. A glass slide covered with the OPC to be tested was attached to the microchannel. The inlet of the microchannel was connected to a syringe pump (PHD ULTRA, Harvard Apparatus, USA), and the outlet was attached to a waste reservoir using a Teflon tube. Two pressure taps were installed at the microchannel, and they were connected to a differential manometer (PX409-10WDWUUSBH, Omega engineering, USA). The differential pressure of the two taps was recorded when the channel flow reached a steady-state condition. The pressure drops over the OPC surfaces were measured with varying Reynolds number to examine the frictional drag reduction rate of the fabricated OPC surfaces. The drag forces exerted on the pristine PDMS and glass surfaces were also measured to compare with the drag reduction effect of oleamide.[40]

4.6. Anti-Biofouling Properties. The antialgal spore adhesion test was conducted to evaluate the anti-biofouling properties of the fabricated OPC surfaces. The multistep anti-biofouling experiment process is illustrated in Figure S2. Red alga (*P. yezoensis*) was incubated in the Provasoli's enriched seawater (PES) medium at 10 °C under 50 μmol photons m^{-2} s^{-1} (12L:12D).[41] For the antifouling experiments, the monospore-induced *P. yezoensis* was strongly vortexed in the PES medium, and the spores were released. The released spores were filtered through a 40 μm nylon filter to screen cell debris and unexposed spores. Afterward, the supernatant, excluding spore pellets, was collected and added with new PES medium treated at 10 °C for 5 min in a centrifuge (UNION32R, Hanil Scientific Inc.) rotating at 300 rpm. This process was repeated thrice to wash off the exfoliations and bacterial spores. The concentration of spores was measured using a hemocytometer and diluted to 4 × 10^5 mL^{-1}. The spores (5 mL) were distributed into a six-well plate. After 24 h of incubation at 10 °C, the spores were replaced with a new medium after stirring at 100 rpm for 5 min. Thereafter, the nonadhesive spores were washed. The observation was conducted after incubation at 10 °C under 50 μmol photons m^{-2} s^{-1} for three weeks.[42]

The algal spores were observed using a stereomicroscope (Olympus SZX10, Olympus, Tokyo, Japan) attached with an IP camera (ip-8000; Hanwha Techwin, Changwon-si, Korea). The ImageJ program was used to analyze the number of attached spores. The mean diatom cells were calculated from three replicates, and the results were expressed as mean (±SD).

4.7. Mussel Antifouling Assay. The mussel adhesion performance was measured to evaluate the anti-biofouling properties of mussels on the fabricated OPC surfaces. Fresh mussels were collected from the East Sea in front of Pohang, Korea. A tank was filled with seawater. A polystyrene Petri dish of 90 mm diameter, a Petri dish coated with PDMS, and a Petri dish coated with OPC 20:1 (heated for 6 or 24 h at 60 °C) were collectively placed into the tank. The movements of mussel bodies and feet were observed at room temperature for more than 16 h.

■ ASSOCIATED CONTENT

Supporting Information

The Supporting Information is available free of charge at https://pubs.acs.org/doi/10.1021/acsomega.0c00633.

Fabrication of the OPC surface by mixing oleamide and PDMS solution and anti-biofouling experiment using algal spores (PDF)

Interaction of the mussels with the floor surface (MP4)

■ AUTHOR INFORMATION

Corresponding Author

Sang Joon Lee − *Department of Mechanical Engineering, Pohang University of Science and Technology (POSTECH), Pohang 37673, South Korea;* orcid.org/0000-0003-3286-5941; Phone: (82)-054-279-2169; Email: sjlee@postech.ac.kr

Authors

Eunseok Seo − *Department of Mechanical Engineering, Pohang University of Science and Technology (POSTECH), Pohang 37673, South Korea*

Myeong Ryun Seong − *Department of Mechanical Engineering, Pohang University of Science and Technology (POSTECH), Pohang 37673, South Korea*

Ji Woong Lee − *Department of Biological Sciences, Kongju National University, Gongju 314-701, South Korea*

Heejin Lim − *Department of New Biology, DGIST (Daegu Gyeongbuk Institute of Science and Technology), Daegu 711-873, South Korea*

Jiwon Park − *Department of Microbiology, Chungbuk National University, Cheongju 28644, South Korea*

https://dx.doi.org/10.1021/acsomega.0c00633
ACS Omega 2020, 5, 11515−11521

Hyungbin Kim − *Division of Integrative Biosciences and Biotechnology (IBB), Pohang University of Science and Technology (POSTECH), Pohang 37673, South Korea*
Hyundo Hwang − *Department of Mechanical Engineering, Pohang University of Science and Technology (POSTECH), Pohang 37673, South Korea*
Dohoon Lee − *Division of Environmental Science and Engineering, Pohang University of Science and Technology (POSTECH), Pohang 37673, South Korea*
Jiho Kim − *Pohang Accelerator Laboratory, Pohang 37673, South Korea*
Gwang Hoon Kim − *Department of Biological Sciences, Kongju National University, Gongju 314-701, South Korea*
Dong Soo Hwang − *Division of Environmental Science and Engineering, Pohang University of Science and Technology (POSTECH), Pohang 37673, South Korea;* orcid.org/0000-0002-2487-2255

Complete contact information is available at: https://pubs.acs.org/10.1021/acsomega.0c00633

Notes

The authors declare no competing financial interest.

■ ACKNOWLEDGMENTS

Kyunghum Baek is acknowledged for the valuable help in the SEM imaging experiment conducted at the SEM laboratory of the NINT. The authors are also grateful to the staffs and supporting groups of the 12D X-ray Biomedical Imaging Beamline of the Pohang Light Source (Pohang, Korea) for their assistance during the X-ray imaging experiments. This work was supported by the National Research Foundation (NRF) of Korea Grant funded by the Korean Government (MSIP) (no. 2019M3C1B7025088).

■ REFERENCES

(1) Yebra, D. M.; Kiil, S.; Dam-Johansen, K. Antifouling technology - past, present and future steps towards efficient and environmentally friendly antifouling coatings. *Prog. Org. Coat.* **2004**, *50*, 75−104.
(2) Yin, K.; Dong, X.; Zhang, F.; Wang, C.; Duan, J. a. Superamphiphobic miniature boat fabricated by laser micromachining. *Appl. Phys. Lett.* **2017**, *110*, 121909.
(3) Tulcidas, A. V.; Bayón, R.; Igartua, A.; Bordado, J. C. M.; Silva, E. R. Friction reduction on recent non-releasing biocidal coatings by a newly designed friction test rig. *Tribol. Int.* **2015**, *91*, 140−150.
(4) Bai, X. Q.; Xie, G. T.; Fan, H.; Peng, Z. X.; Yuan, C. Q.; Yan, X. P. Study on biomimetic preparation of shell surface microstructure for ship antifouling. *Wear* **2013**, *306*, 285−295.
(5) Müller, W.; Wang, X.; Guo, Y.-W.; Schröder, H. Potentiation of the cytotoxic activity of copper by polyphosphate on biofilm-producing bacteria: a bioinspired approach. *Mar. Drugs* **2012**, *10*, 2369−2387.
(6) Müller, W. E. G.; Wang, X.; Proksch, P.; Perry, C. C.; Osinga, R.; Gardères, J.; Schröder, H. C. Principles of biofouling protection in marine sponges: a model for the design of novel biomimetic and bio-inspired coatings in the marine environment? *Mar. Biotechnol.* **2013**, *15*, 375−398.
(7) Bixler, G. D.; Bhushan, B. Biofouling: lessons from nature. *Philos. Trans. R. Soc., A* **2012**, *370*, 2381−2417.
(8) Logan, K. P. Using a Ship's Propeller for Hull Condition Monitoring. *Nav. Eng. J.* **2012**, *124*, 71−87.
(9) Townsin, R. L. The Ship Hull Fouling Penalty. *Biofouling* **2003**, *19*, 9−15.
(10) Cloutier, M.; Mantovani, D.; Rosei, F. Antibacterial Coatings: Challenges, Perspectives, and Opportunities. *Trends Biotechnol.* **2015**, *33*, 637−652.
(11) Bandara, C. D.; Singh, S.; Afara, I. O.; Wolff, A.; Tesfamichael, T.; Ostrikov, K.; Oloyede, A. Bactericidal Effects of Natural Nanotopography of Dragonfly Wing on Escherichia coli. *ACS Appl. Mater. Interfaces* **2017**, *9*, 6746−6760.
(12) Jeong, H. E.; Kim, I.; Karam, P.; Choi, H.-J.; Yang, P. Bacterial recognition of silicon nanowire arrays. *Nano Lett.* **2013**, *13*, 2864−2869.
(13) Bhadra, C. M.; Truong, V. K.; Pham, V. T.; Al Kobaisi, M.; Seniutinas, G.; Wang, J. Y.; Juodkazis, S.; Crawford, R. J.; Ivanova, E. P. Antibacterial titanium nano-patterned arrays inspired by dragonfly wings. *Sci. Rep.* **2015**, *5*, 16817.
(14) Ivanova, E. P.; Hasan, J.; Webb, H. K.; Gervinskas, G.; Juodkazis, S.; Truong, V. K.; Wu, A. H.; Lamb, R. N.; Baulin, V. A.; Watson, G. S.; Watson, J. A.; Mainwaring, D. E.; Crawford, R. J. Bactericidal activity of black silicon. *Nat. Commun.* **2013**, *4*, 2838.
(15) Atanasov, A. G.; Nashev, L. G.; Tam, S.; Baker, M. E.; Odermatt, A. Organotins disrupt the 11beta-hydroxysteroid dehydrogenase type 2-dependent local inactivation of glucocorticoids. *Environ. Health Perspect.* **2005**, *113*, 1600−1606.
(16) Scardino, A. J.; de Nys, R. Mini review: Biomimetic models and bioinspired surfaces for fouling control. *Biofouling* **2011**, *27*, 73−86.
(17) Minchin, D.; Stroben, E.; Oehlmann, J.; Bauer, B.; Duggan, C. B.; Keatinge, M. Biological indicators used to map organotin contamination in Cork Harbour, Ireland. *Mar. Pollut. Bull.* **1996**, *32*, 188−195.
(18) Sonak, S. Implications of organotins in the marine environment and their prohibition. *J. Environ. Manage.* **2009**, *90*, S1−S3.
(19) Wang, P.; Zhang, D.; Lu, Z. Slippery liquid-infused porous surface bio-inspired by pitcher plant for marine anti-biofouling application. *Colloids Surf., B* **2015**, *136*, 240−247.
(20) Manna, U.; Raman, N.; Welsh, M. A.; Zayas-Gonzalez, Y. M.; Blackwell, H. E.; Palecek, S. P.; Lynn, D. M. Slippery Liquid-Infused Porous Surfaces that Prevent Microbial Surface Fouling and Kill Non-Adherent Pathogens in Surrounding Media: A Controlled Release Approach. *Adv. Funct. Mater.* **2016**, *26*, 3599−3611.
(21) Chen, R.; Li, Y.; Tang, L.; Yang, H.; Lu, Z.; Wang, J.; Liu, L.; Takahashi, K. Synthesis of zinc-based acrylate copolymers and their marine antifouling application. *RSC Adv.* **2017**, *7*, 40020−40027.
(22) Chen, R.; Li, Y.; Yan, M.; Sun, X.; Han, H.; Li, J.; Wang, J.; Liu, L.; Takahashi, K. Synthesis of hybrid zinc/silyl acrylate copolymers and their surface properties in the microfouling stage. *RSC Adv.* **2016**, *6*, 13858−13866.
(23) Callow, J. A.; Callow, M. E. Trends in the development of environmentally friendly fouling-resistant marine coatings. *Nat. Commun.* **2011**, *2*, 244.
(24) Gudipati, C. S.; Finlay, J. A.; Callow, J. A.; Callow, M. E.; Wooley, K. L. The Antifouling and Fouling-Release Perfomance of Hyperbranched Fluoropolymer (HBFP)−Poly(ethylene glycol) (PEG) Composite Coatings Evaluated by Adsorption of Biomacromolecules and the Green Fouling Alga Ulva. *Langmuir* **2005**, *21*, 3044−3053.
(25) Yang, R.; Jang, H.; Stocker, R.; Gleason, K. K. Synergistic prevention of biofouling in seawater desalination by zwitterionic surfaces and low-level chlorination. *Adv. Mater.* **2014**, *26*, 1711−1718.
(26) Yang, W. J.; Neoh, K.-G.; Kang, E.-T.; Teo, S. L.-M.; Rittschof, D. Polymer brush coatings for combating marine biofouling. *Prog. Polym. Sci.* **2014**, *39*, 1017−1042.
(27) Fyrner, T.; Lee, H.-H.; Mangone, A.; Ekblad, T.; Pettitt, M. E.; Callow, M. E.; Callow, J. A.; Conlan, S. L.; Mutton, R.; Clare, A. S.; Konradsson, P.; Liedberg, B.; Ederth, T. Saccharide-functionalized alkanethiols for fouling-resistant self-assembled monolayers: synthesis, monolayer properties, and antifouling behavior. *Langmuir* **2011**, *27*, 15034−15047.
(28) Song, Y.; Liu, M.; Zhang, L.; Mu, C.; Hu, X. Mechanistic interpretation of the curing kinetics of tetra-functional cyclosiloxanes. *Chem. Eng. J.* **2017**, *328*, 274−279.
(29) Song, Y.; Tang, X.; Liang, Y. N.; Lee, H. Y.; Liu, M.; Zhang, L.; Bi, S.; Mu, C.; Hu, X. Bioinspired reinforcement of cyclosiloxane hybrid polymer. *Chem. Commun.* **2018**, *54*, 13415−13418.

(30) Zhang, H.; Chiao, M. Anti-fouling Coatings of Poly-(dimethylsiloxane) Devices for Biological and Biomedical Applications. *J. Med. Biol. Eng.* **2015**, *35*, 143−155.
(31) Yang, K.; Jung, H.; Lee, H.-R.; Lee, J. S.; Kim, S. R.; Song, K. Y.; Cheong, E.; Bang, J.; Im, S. G.; Cho, S.-W. Multiscale, Hierarchically Patterned Topography for Directing Human Neural Stem Cells into Functional Neurons. *ACS Nano* **2014**, *8*, 7809−7822.
(32) Holm, E. R.; Kavanagh, C. J.; Meyer, A. E.; Wiebe, D.; Nedved, B. T.; Wendt, D.; Smith, C. M.; Hadfield, M. G.; Swain, G.; Wood, C. D.; Truby, K.; Stein, J.; Montemarano, J. Interspecific variation in patterns of adhesion of marine fouling to silicone surfaces. *Biofouling* **2006**, *22*, 233−243.
(33) Garrido-López, Á.; Esquiu, V.; Tena, M. T. Determination of oleamide and erucamide in polyethylene films by pressurised fluid extraction and gas chromatography. *J. Chromatogr. A* **2006**, *1124*, 51−56.
(34) Getachew, P.; Getachew, M.; Joo, J.; Choi, Y. S.; Hwang, D. S.; Hong, Y.-K. The slip agents oleamide and erucamide reduce biofouling by marine benthic organisms (diatoms, biofilms and abalones). *Toxicol. Environ. Health Sci.* **2017**, *8*, 341−348.
(35) Mansha, M.; Gauthier, C.; Gerard, P.; Schirrer, R. The effect of plasticization by fatty acid amides on the scratch resistance of PMMA. *Wear* **2011**, *271*, 671−679.
(36) Cho, J.-Y. Antifouling Activity of Giffinisterone B and Oleamide Isolated from a Filamentous Bacterium Leucothrix mucor Culture against Ulva pertusa. *Korean J. Fish. Aquat. Sci.* **2012**, *45*, 30−34.
(37) Chaudhury, M. K.; Finlay, J. A.; Chung, J. Y.; Callow, M. E.; Callow, J. A. The influence of elastic modulus and thickness on the release of the soft-fouling green alga Ulva linza (syn. Enteromorpha linza) from poly(dimethylsiloxane) (PDMS) model networks. *Biofouling* **2005**, *21*, 41−48.
(38) Chae, B.; Hong, D. G.; Jung, Y. M.; Won, J. C.; Lee, S. W. Investigation of phase separated polyimide blend films containing boron nitride using FTIR imaging. *Spectrochim. Acta, Part A* **2018**, *195*, 1−6.
(39) Chen, Z.; Zhou, K.; Lu, X.; Lam, Y. C. A review on the mechanical methods for evaluating coating adhesion. *Acta Mech.* **2013**, *225*, 431−452.
(40) Lee, S. J.; Kim, H. N.; Choi, W.; Yoon, G. Y.; Seo, E. Correction: A nature-inspired lubricant-infused surface for sustainable drag reduction. *Soft Matter* **2019**, *15*, 8640.
(41) Starr, R. C.; Zeikus, J. A. Utex-the Culture Collection of Algae at the University of Texas at Austin 1993 List of Cultures1. *J. Phycol.* **1993**, *29*, 1−106.
(42) Klochkova, T. A.; Kang, S.-H.; Cho, G. Y.; Pueschel, C. M.; West, J. A.; Kim, G. H. Biology of a terrestrial green alga, Chlorococcum sp. (Chlorococcales, Chlorophyta), collected from the Miruksazi stupa in Korea. *Phycologia* **2006**, *45*, 349−358.
(43) Widder, L.; Ristic, A.; Brenner, F.; Brenner, J.; Hutter, H. Modified-Atmospheric Pressure-Matrix Assisted Laser Desorption/Ionization Identification of Friction Modifier Additives Oleamide and Ethoxylated Tallow Amines on Varied Metal Target Materials and Tribologically Stressed Steel Surfaces. *Anal. Chem.* **2015**, *87*, 11375−11382.
(44) Moreno-Couranjou, M.; Mauchauffé, R.; Bonot, S.; Detrembleur, C.; Choquet, P. Anti-biofouling and antibacterial surfaces via a multicomponent coating deposited from an up-scalable atmospheric-pressure plasma-assisted CVD process. *J. Mater. Chem. B* **2018**, *6*, 614−623.
(45) Aldred, N.; Li, G.; Gao, Y.; Clare, A. S.; Jiang, S. Modulation of barnacle (Balanus amphitrite Darwin) cyprid settlement behavior by sulfobetaine and carboxybetaine methacrylate polymer coatings. *Biofouling* **2010**, *26*, 673−683.

https://dx.doi.org/10.1021/acsomega.0c00633
ACS Omega 2020, 5, 11515−11521